24th COBEM - 2017

24th ABCM International Congress of Mechanical Engineering
December 3-8, 2017, Curitiba, PR, Brazil

COBEM-2017-2047
GUST LOAD ALLEVIATION IN A SMART IDEALIZED WING

Thiago de Souza S. Versiani
Flávio J. Silvestre
Antônio B. Guimarães Neto
Domingos A. Rade
Roberto G. Annes da Silva
Rafael M. Bertolin
Gefferson C. Silva
Pedro J. G. Ramirez
Instituto Tecnológico de Aeronáutica, Marechal Eduardo Gomes Square, 50, Vila das Acácias, São José dos Campos − SP, Brazil
versiani.t@gmail.com
flaviojs@ita.com
antoniobgn@gmail.com
rade@ita.br
gil@ita.br
rafaelmbufsj@gmail.com
geffersonports@hotmail.com
pedrojgonzalezr@gmail.com

Abstract. *Among the aeroelastic phenomena that affect flexible and very flexible aircraft, those caused by gusts deserve special attention due to their potential in increasing structural loads and decreasing flying qualities. In this work, the gust load alleviation on a smart idealized wing by active, model-based control is analyzed and experimentally tested in a wind-tunnel facility. The results show a considerable attenuation of the wing root bending moment by decreasing the amplitude of oscillations resulting from gust disturbances, especially at the frequency of the wing's first bending moment via feedback of observed output.*

Keywords: *aeroservoelasticity, gust load alleviation, smart materials*

1. INTRODUCTION

Recent aircraft, for both military and civil applications, are getting more flexible, especially due to the attempt of increasing the performance while decreasing weight. Flexible aircraft are very sensible to gust loads which could result in degradation handling qualities (Klemin, 1936; Rockefeller, 1936; Abdelmoula, 1999) or even structural damage or failure (Noll *et al.*, 2004). Conventional strategies of gust load alleviation generally use heavy devices, so alternative solutions have been developed trough the use of special actuators (Moulin and Karpel, 2007) and of passive and active control (Zeng *et al.*, 2012; Haghighat *et al.*, 2012; Mattaboni *et al.*, 2012; Bernhammer *et al.*, 2014; Wang and Inman, 2012; Agneni *et al.*, 2002; Tsushima and Su, 2016; Alam *et al.*, 2015).

Structural vibration with the use of piezoelectric transducers is already investigated and is commonly found in literature (Abreu, 2003; Fuller *et al.*, 1996; Dimitriadis *et al.*, 1991). Specially for aeroelastic control, the piezoelectric transducers can be applied as a passive control application in order to increase stabilization, due to its intrinsic capacity to transform mechanical energy into electrical energy. Agneni et al. (2002) applied piezoelectric actuators in a glider wing and verified a weak capability of improving the stability margin, except around the natural frequencies, where a displacement attenuation up to 130 dB was gotten for the third mode. Bruni et al. (2014) evaluated the amount of power density harvested via electric circuit and got up to 20% of reduction of dynamic oscillation by increasing the associated electrical resistance in 1×10^5 Ohm; Wang and Inman (2012), in turn, evaluated the energy harvested and spent by the electronic devices embedded on a aeroelastic system. A reduction of 16 dB of tip displacement of the first elastic mode and a control energy decrease up to 76% using the proposed Reduced Energy Control (REC) were verified. By the results obtained in a previous work, a good performance of passive control using piezoelectric transducers is obtained specially around the natural frequencies of the aeroelastic system under study. In spite of the advantages in weight and electronic complexity of embedding passive control devices using piezoelectric transducers, the use of active control systems is encouraged to provide better performance for aeroelastic control.

Into the application of active aeroelastic control, Suleman and Costa (2004) studied the feasibility of applying piezoelectric transducers in order to increase aeroelastic stabilization of a flexible aircraft. The performance of this technological aeroelastic control system, which provided a gust response reduction up to 80%, was compared with the performance of a conventional control surface which, in turn, provided a reduction up to 13%. In both cases, output-based feedback was applied to calculate the gains.

Once the modal states of an aeroelastic system provides specific information about their dynamics, the present work provide a study of an active control system based on observed-output feedback control law compared with the output feedback one applied in an intelligent aeroelastic system using only piezoelectric transducers. The application of both control systems was numerically analyzed and experimentally tested.

2. FORMULATION AND MODEL

The structural model is based on the finite-element method, employing two-node, twelve-degree-of-freedom beam elements, assuming small deformations and neglecting shear effects. Furthermore, the model contains the inertial parcel of the piezoelectric transducers. The aerodynamics is modeled with a quasi-steady strip theory (Silvestre and Luckner, 2015).

The dynamics of the coupled system is represented in modal coordinates by Eq. 1, where $[\mu]$, $[\gamma]$ and $[\beta]$ are the generalized mass, stiffness and damping matrices, respectively; $[\Phi]$ is the matrix of mode shapes, containing the modal displacements at a discrete set of points, for each mode of vibration considered; q_d is the dynamic pressure; $[A_1]$ is an integration matrix that transforms the strips' lift coefficients to elastic axis nodes, forces and moments per unit dynamic pressure; $[A_0]$ is the matrix containing the lift coefficient derivatives related to each strip; $[D_1]$ is the downwash matrix containing the terms that transform elastic-axis rates of displacement to control-point downwashes (the control points are located at 3/4 of each strip chord); $[D_0]$ is the downwash matrix containing the terms that transform elastic-axis displacements to control-point downwashes; $\{D_g\}$ contains the terms that transform the gust speed at each strip to the control-point downwashes, hence being a column unit matrix of length n_{strip}; $[G]$ is the interpolation matrix from the structural to the aerodynamic degrees of freedom; A_{gust} is the amplitude and f_{gust} is the frequency of the normal velocity component of the gust.

$$\begin{aligned}&\{\ddot{\eta}(t)\} + [\mu]^{-1}[\beta]\{\dot{\eta}(t)\} + [\mu]^{-1}[\gamma]\{\eta(t)\} = \\ &q_d[\mu]^{-1}[\Phi]^T[G]^T[A_1][A_0]\left([D_1][G][\Phi]\left(\frac{b}{V}\right)\{\dot{\eta}(t)\} + [D_0][G][\Phi]\{\eta(t)\} + \{D_g\}A_{\text{gust}}\cos(f_{\text{gust}}t)\right).\end{aligned} \tag{1}$$

The model of piezoelectric behavior of the transducers is based on the electromechanical variational principle for piezoelectric materials (Abreu, 2003). The conversion of energy between the mechanical and electrical physical domains is described by the electromechanical coupling matrix, denoted by $[k_{q\phi}]$ and given by Eq. 2, in which $\left[B_q''\right]$ is the axial strain field; $e_{31_{\text{pzt}}}$ is the piezoelectric strain coefficient; $B_z = 1/(h_{\text{pzt}})$, in which h_{pzt} is the thickness of the piezoelectric transducer; and the domain of integration V is the volume of the device.

$$[k_{q\phi}] = \int_V \left(z\left[B_q''\right]\right)^T e_{31_{\text{pzt}}} B_z dV_{\text{pzt}} \tag{2}$$

3. CONTROL DESIGN

The stability augmentation system (SAS) was designed assuming two different control laws: one based on output feedback and other based on observed-output feedback.

3.1 Output feedback

The system under study can be represented by a linear, time-invariant state-space model:

$$\{\dot{x}(t)\} = [A]\{x(t)\} + [B]\{u(t)\} + [W]\,d(t) \tag{3}$$

$$\{y(t)\} = [C]\{x(t)\} \tag{4}$$

where $[A] \in \mathbb{R}^{8\times 8}$ is the state matrix, $[B] \in \mathbb{R}^{8\times 2}$ is the input matrix, $[W] \in \mathbb{R}^{8\times 1}$ is the matrix that determines the effect of the disturbance on the state, $[C] \in \mathbb{R}^{1\times 8}$ is the output matrix, $\{x(t)\} \in \mathbb{R}^{8\times 1}$ is the state vector containing the j-th elastic states $\eta_j(t)$ and its respective time derivative $\dot{\eta}_j(t)$ with $j = 1, \cdots, 4$, $\{u(t)\} \in \mathbb{R}^{2\times 1}$ is the input vector containing the input voltage of the first ($\phi_{a_1}(t)$) and second ($\phi_{a_2}(t)$) PZT actuator, $d(t)$ is the gust disturbance input and $\{y(t)\} \in \mathbb{R}^{1\times 1}$ is the output vector corresponding to filtered voltage of the PVDF sensor ($\phi_s(t)$).

Once the output signal of the PVDF sensor is directly proportional to the wing root bending moment, this signal ($y(t)$) can be used as input of a proportional regulator to produce a control signal ($u(t)$), as illustrated in Fig. 1.

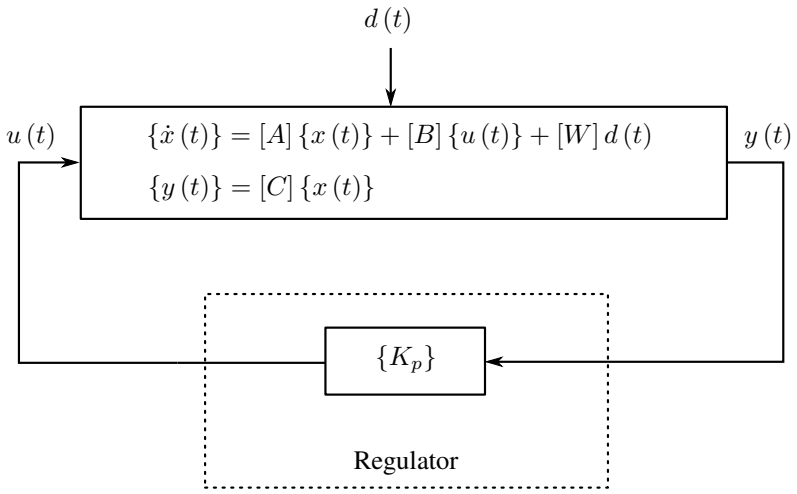

Figure 1. Block-diagram representation of a regulator problem.

Since the problem in hands involves only stabilization, a pure proportional feedback was chosen, resulting in a control law described by:

$$\begin{aligned}\{u(t)\} &= -[K]\{y(t)\} \\ &= -\begin{bmatrix} K_1 \\ K_2 \end{bmatrix}\{\phi_s(t)\},\end{aligned} \tag{5}$$

where the gains K_1 and K_2 could be calculated using a LQR technique by the minimization of the quadratic performance index (J) in the form:

$$J = \frac{1}{2}\int_0^\infty \left[\rho\{y(t)\}^T\{y(t)\} + \{u(t)\}^T[R]\{u(t)\}\right]dt, \tag{6}$$

in which the parameters ρ and $[R]$ penalize the output variable and control energy, respectively.

The closed-loop system can be assumed to be asymptotically stable, so J can be written as:

$$J = \frac{1}{2}tr([P]), \tag{7}$$

in which $[P]$ is a symmetric positive-semidefinite matrix that satisfies the Lyapunov equation:

$$\left([A] - [B][K][C]\right)^T[P] + [P]\left([A] - [B][K][C]\right) + \left([Q] + [C]^T[K]^T[R][K][C]\right) = 0. \tag{8}$$

By the usage of output feedback, the control system was applied using one and two actuators in order to verify the control performance with respect to the number of actuators used. Both cases was tested in a operating condition corresponding to flow velocity of $5.0\ m/s$.

In order to obtain the best trade-off between good performance and required control energy, the parameters was set as $\rho = 1$ and $[R]$ as described at Tab. 1. Then, the proportional gains was obtained as described in Tab. 2.

Table 1. Weighting matrix $[R]$ to each number of actuators.

One PZT	Two PZT
$[R] = \left[1.0 \times 10^{-4}\right]$	$[R] = \begin{bmatrix} 5.5 \times 10^{-6} & 0 \\ 0 & 2.0 \times 10^{-5} \end{bmatrix}$

Table 2. Regulator gain scheduling, $[K]$.

One PZT	Two PZT
$[K] = \begin{bmatrix} 20.9678 \\ 0 \end{bmatrix}$	$[K] = \begin{bmatrix} 64.8416 \\ -54.2994 \end{bmatrix}$

3.2 Observed-output feedback

The state feedback can be used to provide important robustness properties that are not guaranteed using the output feedback (Stevens *et al.*, 2015). Generally, the states in a real system can not be accessed directly, but if the output signal cares enough information about the dynamics of the system, it can be used to estimate the desired states. Based on the gust response of interest, the observation of the reduced order model was applied considering only the states of greater influence on the wing flexible dynamics. Then, since the problem proposed is to reduce the wing root bending moment, an observer was designed to estimate the states of the first and second elastic modes.

Therefore, consider the state-space of the full-order model described by Eq. 3 and 4, and rearranged as follow:

$$\{\dot{x}(t)\} = [A]\{x(t)\} + \overbrace{[B \quad W]}^{[B_d]} \overbrace{\begin{Bmatrix} u(t) \\ d(t) \end{Bmatrix}}^{\{u_d(t)\}} \tag{9}$$

$$\{y(t)\} = [C]\{x(t)\} \tag{10}$$

The reduced-order model obtained through a full-order model truncation is:

$$\big\{\dot{x}_r(t)\big\} = \big[A_r\big]\big\{x_r(t)\big\} + \big[B_r\big]\big\{u_d(t)\big\} \tag{11}$$

$$\big\{y_r(t)\big\} = \big[C_r\big]\big\{x_r(t)\big\} \tag{12}$$

where $\big[A_r\big] \in \mathbb{R}^{4\times4}$ is the reduced state matrix, $\big[B_r\big] \in \mathbb{R}^{4\times3}$ is the reduced input matrix and $\big[C_r\big] \in \mathbb{R}^{1\times4}$ is the reduced output matrix. The reduced state vector $\big\{x_r(t)\big\} \in \mathbb{R}^{4\times1}$ is given by:

$$\big\{x_r(t)\big\} = \begin{Bmatrix} \eta_1(t) & \eta_2(t) & \dot{\eta}_1(t) & \dot{\eta}_2(t) \end{Bmatrix}^T \tag{13}$$

The input vector is now $\big\{u_d(t)\big\} \in \mathbb{R}^{3\times1}$ and the reduced output vector is $\big\{y_r(t)\big\} \in \mathbb{R}^{1\times1}$. Although the system in question presents only one output, it captures enough information to estimate the dynamics of the plant, since $\big\{y_r(t)\big\}$ is a linear combination of the modal amplitudes.

Let the estimate of $x_r(t)$ be $\hat{x}_r(t)$. The state observer here proposed is a dynamical system described by (Silvestre *et al.*, 2017):

$$\big\{\dot{\hat{x}}_r(t)\big\} = \big[A_r\big]\big\{\hat{x}_r(t)\big\} + \big[B_r\big]\big\{u_d(t)\big\} + \big[L\big]\Big(\big\{y_r(t)\big\} - \big\{\hat{y}_r(t)\big\}\Big) \tag{14}$$

$$\big\{\hat{y}_r(t)\big\} = \big[C_r\big]\big\{\hat{x}_r(t)\big\} \tag{15}$$

where $\big\{\hat{y}_r(t)\big\}$ is the reduced estimated output and $\big[L\big]$ the observer gain.

Looking at the Eq. 14 and 15, it is noticed that if the observer is working propely, the output estimation error defined as:

$$\big\{\tilde{y}(t)\big\} = \big\{y_r(t)\big\} - \big\{\hat{y}_r(t)\big\} \tag{16}$$

should be small and the observer proposed will behave like the reduced-order model give by 11 and 12. It means that the signals $\big\{\hat{x}_r(t)\big\}$ approach $\big\{x_r(t)\big\}$ and that the state estimation error defined as:

$$\big\{\tilde{x}(t)\big\} = \big\{x_r(t)\big\} - \big\{\hat{x}_r(t)\big\} \tag{17}$$

tends to vanish. Therefore, the observer design problem is to select $\big[L\big]$ so that the estimation error dynamic, given by:

$$\begin{aligned} \big\{\dot{\tilde{x}}(t)\big\} &= \big(\,[A_r] - [L]\,[C_r]\,\big)\big\{\tilde{x}(t)\big\} \\ &= \big[A_o\big]\big\{\tilde{x}(t)\big\} \end{aligned} \tag{18}$$

be asymptotically stable. Equation 18 is obtained by differentiating Eq. 17 and using Eq. 11 and 14.

It is known from the literature Stevens *et al.* (2015) that the poles of $\big[A_o\big]$ may be arbitrarily assigned to desired location if and only if the system is observable, it means, $\big(\,[A_r]\,,[C_r]\,\big)$ should have full rank $(=4)$ considering the model of the operating condition ($V = 5\ m/s$), as is the case. Thus, the observer gain matrix can be calculated using the state feedback $\big\{\tilde{x}(t)\big\}$ linear quadratic regulator via the Riccati equation (Silvestre *et al.*, 2017).

Choosing weighting matrices $50I_4$ for $\{\tilde{x}(t)\}$ and 1 for $\{\tilde{y}(t)\}$, then solving the associated Riccati equation, the observer gain matrices L calculated is:

$$L = \begin{bmatrix} -6.8445 \\ 6.4583 \\ 23.7832 \\ 344.2186 \end{bmatrix} \tag{19}$$

Uncoupled control was chosen to be applied to the aeroservoelastic system, in order to dedicate one actuator to each state and evaluate their contribution to the gust load alleviation. So on, the η_1 state was set to the first actuator (nearest to the base) and the $\dot{\eta}_1$ state was set to the second one.

The gain of the η_1 loop was calculated by the minimization of a performance index which integrates the square of the output signal, i.e. PVDF signal, in order to lead the moment at the root of the wing to zero, as described at the Eq. 20.

$$J = \int_{t_1}^{t_2} \left(\phi\left(t\right)\right)^2 dt \tag{20}$$

The parameters of this performance index was the augmented matrices of the system counting the observer dynamics, the amplitude and frequency of the gust disturbance (1 Hz and 2 Hz) and the time interval of integration, which would be the same of that applied to experimental tests ($\Delta t = 40\ sec.$). So, the contribution of this state to this gust load alleviation problem could be evaluated by its performance.

With the η_1 feedback loop gain in hands, the root locus methodology was used to calculate the $\dot{\eta}_1$ feedback gain and the closed-loop system was obtained closing the η_1 loop first and then the $\dot{\eta}_1$ after. So, the gain that provides the major damp to the first flexible mode, for each point of operation, could be calculated graphically.

Finally, the gain matrices for observed-output feedback control are:

$$[K] = \begin{bmatrix} -600 & 0 \\ 0 & -40 \end{bmatrix} \tag{21}$$

4. EXPERIMENTAL PROCEDURE

The aeroservoelastic system under study is a flat plate-like wing, containing a slender body on its free tip, two PZT actuators attached on one surface and a PVDF sensor on the other one, as illustrated in Fig. 2.

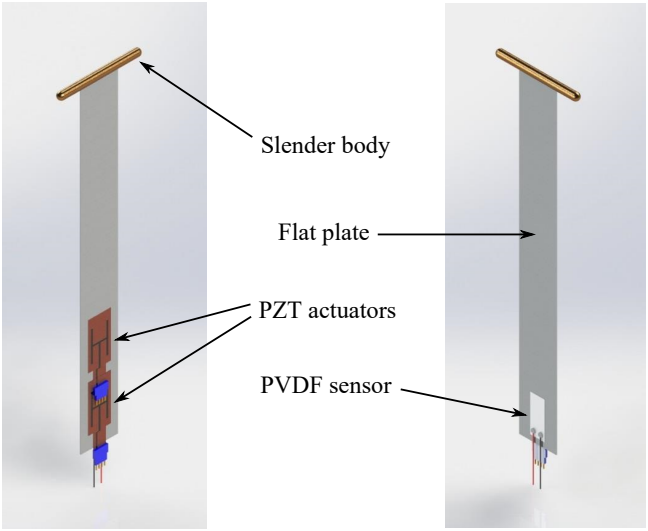

Figure 2. Aeroservoelastic system components.

The idealized wing is clamped to an inertial base in vertical position and presenting no mean angle of attack. At a wind tunnel, the wing is subjected to wind velocity of $V_\infty = 5.0\ m/s$. As can be seen in Fig. 3, a gust generator was mounted in the tunnel to perform changes in wind flow direction and generates sinusoidal vertical gust with 1.0 Hz and 2.0 Hz of frequency of oscillation.

A *dSPACE 1103 Data Acquisition System* was used to process the input/output signals and to apply the control law. The I/O modules support a voltage signal up to $\pm 10\ V$.

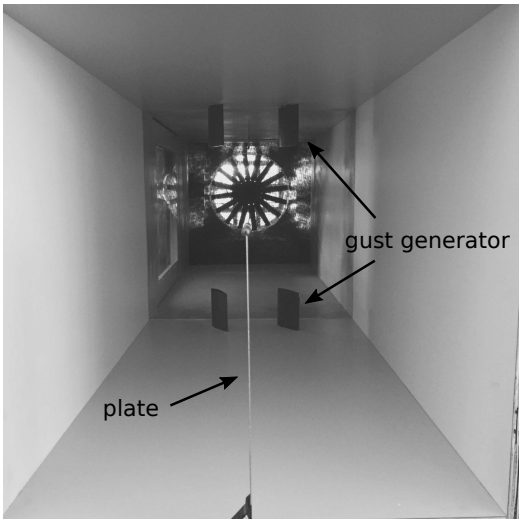

Figure 3. Wind tunnel with gust generator section and the flat plate.

As shown in Fig. 4, an *ACX Quickpack Power Amplifier* (Amp_a) was used to amplify the control signal from the dSPACE to the PZT actuator, which works nominally about $\pm 200\ V$. So, an amplification gain about 20 was set.

To amplify the signal from the PVDF sensor, a *Measurement Specialties Piezo Film Lab Amplifier* (Amp_s) was used in order to set the output voltage signal in the same order of the dSPACE input signal ($\pm 10\ V$). This amplifier contains a multi-pole band-pass filter with the cutoff frequencies at 0.1 Hz and 10 Hz.

Still in the Fig. 4, the subsystem I represents the flat plate with piezoelectric transducers illustrated in Fig. 2 and the subsystem II represents the system described by Eq. 3 and 4 and illustrated in the Fig. 1.

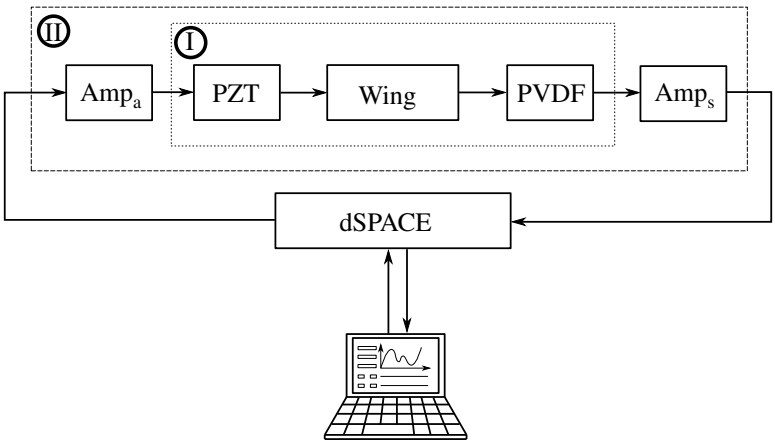

Figure 4. Block diagrams of the experimental setup.

5. RESULTS AND DISCUSSION

Tests were performed for each case of number of actuators, employed control law and disturbance frequency of oscillation. The maximum reduction detected for each case of disturbance mode and first elastic mode is described in

Table 3. Maximum reduction of disturbance mode.

	OF[1] **1 actuator**		**OF 2 actuator**		**SF**[2] **Uncoupled control**	
	%	σ[3]	%	σ	%	σ
$V = 5$, $f_{\text{gust}} = 1$Hz	45	14.1	52	8.8	65	12.8
$V = 5$, $f_{\text{gust}} = 2$Hz	47.7	13	68	15.1	35	9.8

[1] *Output feedback*

[2] *State feedback*

[3] *Standard deviation (%)*

Table 4. Maximum reduction of fist elastic mode.

	OF[1] **1 actuator**		**OF 2 actuator**		**SF**[2] **Uncoupled control**	
	%	σ[3]	%	σ	%	σ
$V = 5$, $f_{\text{gust}} = 1$Hz	7	43.1	70	26.9	90, 7	3.4
$V = 5$, $f_{\text{gust}} = 2$Hz	15	74.6	65	17.88	87.5	4

[1] *Output feedback*
[2] *State feedback*
[3] *Standard deviation (%)*

Tables 3 and 4, respectively. The output observation technique will be referred here as state feedback.

As can be seen at the Tab. 3 and 4, there is a tendency of getting more reduction of oscillation of disturbance influence and first bending mode when using multiple actuators for both control laws tested, with better performance offered by the output-observation technique, except in the reduction of disturbance mode when the gust frequency is $f_{\text{gust}} = 2\ Hz$. In Fig. 5 and 6, time and frequency responses of wing bending moment in both open and closed-loop applying output feedback, for one and two actuators are shown, and the performance improvement using multiple actuators is evident, as expected. In Fig. 7, open and closed-loop responses applying the output-observation technique is shown. Comparing to Fig. 5 and 6, the latter technique is more efficient for wing bending moment reduction at both frequencies (65% reduction at gust excitation frequency and 90.7% reduction at the frequency of first aeroelastic wing mode). The achieved results with the latter technique are encouraging for applications in very flexible aircraft.

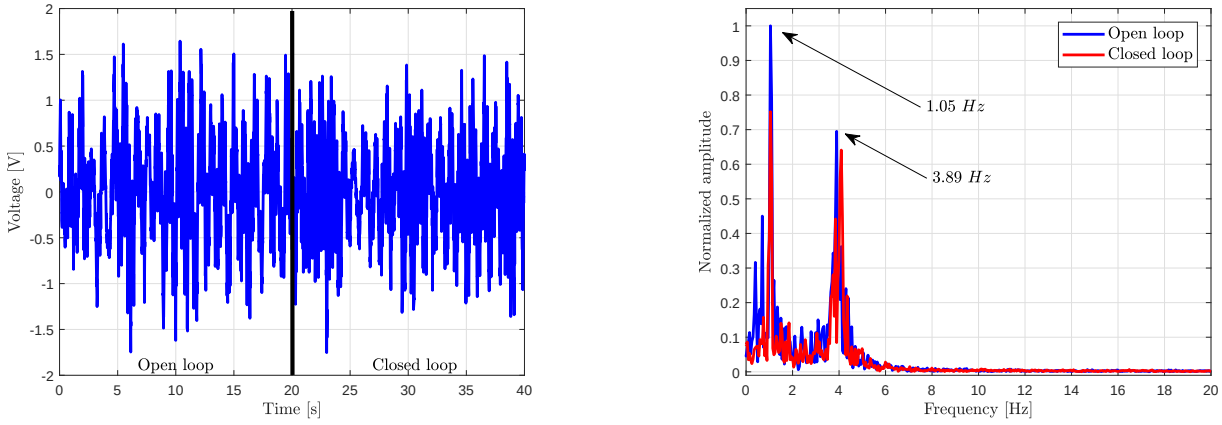

(a) Time response (b) Frequency response

Figure 5. Output feedback - $V = 5\ m/s$, $f_{\text{gust}} = 1\ Hz$ and 1 actuator.

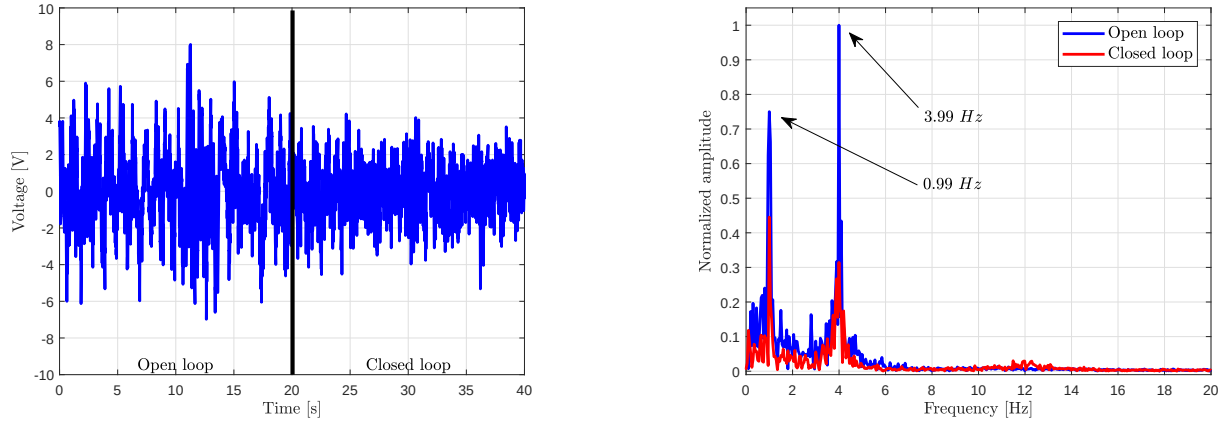

(a) Time response (b) Frequency response

Figure 6. Output feedback - $V = 5\ m/s$, $f_{\text{gust}} = 1\ Hz$ and 2 actuators.

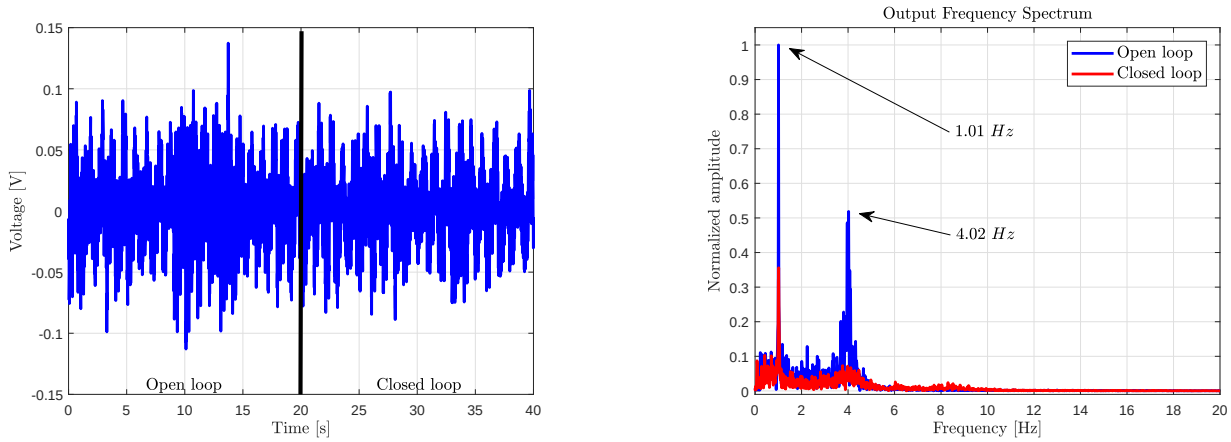

(a) Time response (b) Frequency response

Figure 7. Observed-output feedback - $V = 5\ m/s$, $f_{\text{gust}} = 1\ Hz$.

6. CONCLUSIONS

The gust load alleviation of a smart flexible plate-like wing via active control was presented. The performance of the gust load alleviation system was analyzed for different techniques: a standard output feedback and a novel technique based on observed-output feedback. While the use of two actuators is more efficient than one actuator as expected, and shows considerable reductions of at least 52% of the wing root bending deformation, the observation of truncated state can achieve up to 90.7% of load reduction at the wing first elastic mode, while slightly increasing performance in the gust frequency.

The use of the novel technique based on observed-output feedback showed to be promising for gust load alleviation in smart flexible structures and encourages a more detailed investigation.

7. ACKNOWLEDMENTS

The authors also would like to express special thanks to Prof. Luiz C. Sandoval Góes for providing the data acquisition system.

8. REFERENCES

Abdelmoula, F., 1999. "Design of an open-loop gust alleviation control system for airborne gravimetry". *Aerospace science and technology*, Vol. 3, No. 6, pp. 379–389.

Abreu, G.L.C.M., 2003. *Projeto robusto H_∞ aplicado no controle de vibrações em estruturas flexíveis com materiais piezelétricos incorporados*. Ph.D. thesis, Tese de Doutorado, Universidade Federal de Uberlândia, 265p.

Agneni, A., Mastroddi, F. and Polli, G.M., 2002. "Shunted piezoelectric patches in elastic and aeroelastic vibrations". *Computers & Structures*, Vol. 81, No. 2, pp. 91–105.

Alam, M., Hromcik, M. and Hanis, T., 2015. "Active gust load alleviation system for flexible aircraft: Mixed feedforward/feedback approach". *Aerospace Science and Technology*, Vol. 41, pp. 122–133.

Bernhammer, L.O., Teeuwen, S.P.W., De Breuker, R., van der Veen, G.J. and van Solingen, E., 2014. "Gust load alleviation of an unmanned aerial vehicle wing using variable camber". *Journal of Intelligent Material Systems and Structures*, Vol. 25, No. 7, pp. 795–805.

Bruni, C., Cestino, E., Frulla, G. and Marzocca, P., 2014. "Development of an aeroelastic wing model with piezoelectric elements for gust load alleviation and energy harvesting". In *ASME 2014 International Mechanical Engineering Congress and Exposition*. American Society of Mechanical Engineers.

Dimitriadis, E., Fuller, C. and Rogers, C., 1991. "Piezoelectric actuators for distributed vibration excitation of thin plates". *Journal of Vibration and Acoustics*, Vol. 113, No. 1, pp. 100–107.

Fuller, C.C., Elliott, S. and Nelson, P.A., 1996. *Active control of vibration*. Academic Press.

Haghighat, S., T. Liu, H.H. and RA Martins, J.R., 2012. "Model-predictive gust load alleviation controller for a highly flexible aircraft". *Journal of Guidance, Control, and Dynamics*, Vol. 35, No. 6, pp. 1751–1766.

Klemin, A., 1936. "Stability and control research". *Journal of the Aeronautical Sciences*, Vol. 3, No. 5, pp. 174–175.

Mattaboni, M., Masarati, P., Quaranta, G. and Mantegazza, P., 2012. "Multibody simulation of integrated tiltrotor flight mechanics, aeroelasticity and control". *Journal of Guidance, Control, and Dynamics*, Vol. 35, No. 5, pp. 1391–1405.

Moulin, B. and Karpel, M., 2007. "Gust loads alleviation using special control surfaces". *Journal of Aircraft*, Vol. 44,

No. 1, pp. 17–25.

Noll, T.E., Brown, J.M., Perez-Davis, M.E., Ishmael, S.D., Tiffany, G.C. and Gaier, M., 2004. "Investigation of the Helios prototype aircraft mishap volume I - Mishap Report". *NASA Technical Reports Server - Langley Research Center*, Vol. 9.

Rockefeller, W., 1936. "High altitude transport". *Journal of the Aeronautical Sciences*, Vol. 3, No. 7, pp. 234–236.

Silvestre, F.J., Guimarães Neto, A.B., Bertolin, R.M., da Silva, R.G.A. and Paglione, P., 2017. "Aircraft control based on flexible aircraft dynamics". *Journal of Aircraft*, Vol. 54, No. 1, pp. 262–271.

Silvestre, F.J. and Luckner, R., 2015. "Experimental validation of a flight simulation model for slightly flexible aircraft". *AIAA Journal*, Vol. 53, No. 12, pp. 3620–3636.

Stevens, B.L., Lewis, F.L. and Johnson, E.N., 2015. *Aircraft Control and Simulation: Dynamics, Controls Design, and Autonomous Systems*. John Wiley & Sons.

Suleman, A. and Costa, A.P., 2004. "Adaptive control of an aeroelastic flight vehicle using piezoelectric actuators". *Computers & structures*, Vol. 82, No. 17, pp. 1303–1314.

Tsushima, N. and Su, W., 2016. "Active piezoelectric actuation and control of highly flexible multifunctional wings". *57th AIAA/ASCE/AHS/ASC Structures, Structural Dynamics, and Materials Conference*, p. 0715.

Wang, Y. and Inman, D.J., 2012. "Simultaneous energy harvesting and gust alleviation for a multifunctional composite wing spar using reduced energy control via piezoceramics". *Journal of Composite Materials*, Vol. 47, pp. 125–146.

Zeng, J., Kukreja, S. and Moulin, B., 2012. "Experimental model-based aeroelastic control for flutter suppression and gust-load alleviation". *Journal of Guidance, Control, and Dynamics*, Vol. 35, No. 5, pp. 1377–1390.

9. RESPONSIBILITY NOTICE

The authors are the only responsible for the printed material included in this paper.